

Supplementary Materials for

PUMA and BIM Are Required for Oncogene Inactivation–Induced Apoptosis

Gregory R. Bean, Yogesh Tengarai Ganesan, Yiyu Dong, Shugaku Takeda, Han Liu, Po M. Chan, Yafen Huang, Lewis A. Chodosh, Gerard P. Zambetti, James J.-D. Hsieh, Emily H.-Y. Cheng*

*Corresponding author. E-mail: chenge1@mskcc.org

Published 26 March 2013, *Sci. Signal.* **6**, ra20 (2013)

DOI: 10.1126/scisignal.2003483

The PDF file includes:

- Fig. S1. Immunoblot analysis of siRNA-mediated knockdown of *BIM* and *PUMA*.
- Fig. S2. Immunoblot analysis of siRNA-mediated knockdown.
- Fig. S3. Regulation of ERK and AKT phosphorylation by constitutively active AKT and MEK.
- Fig. S4. Inhibition of lapatinib-mediated induction of *PUMA* mRNA by Myr-AKT.
- Fig. S5. Inhibition of ERK and AKT phosphorylation by various kinase inhibitors.
- Fig. S6. *PUMA* is required for GDC0941-induced apoptosis of BT474 cells.
- Fig. S7. *BIM* mRNA is induced upon treatment with tyrosine kinase inhibitors.
- Fig. S8. Knockdown of p53 fails to prevent lapatinib-mediated *PUMA* induction and apoptosis.
- Fig. S9. *BIM* and *PUMA* are activated upon erlotinib-induced apoptosis of PC9 cells.
- Fig. S10. Immunoblot analysis of HER2 in HER2/Neu-driven mammary tumors.
- Fig. S11. Immunoblot analysis of *BIM* and *PUMA* in HER2/Neu-driven mammary tumors.
- Fig. S12. Immunoblot analysis of EGFR in the tetracycline-inducible EGFR^{L858R} transgenic mouse model.
- Fig. S13. Immunoblot analysis of *PUMA* in EGFR^{L858R}-driven mouse lung tumors.
- Fig. S14. Immunoblot analysis of phosphorylation of AKT and S6K.
- Fig. S15. Immunoblot analysis of siRNA-mediated knockdown of *PUMA*.

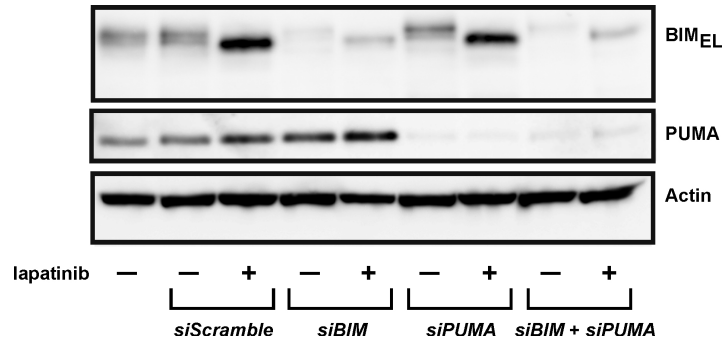


Fig. S1. Immunoblot analysis of siRNA-mediated knockdown of *BIM* and *PUMA*.

BT474 cells transfected with the indicated siRNA were untreated or treated with lapatinib and immunoblotted with the indicated antibodies (n = 2 independent experiments).

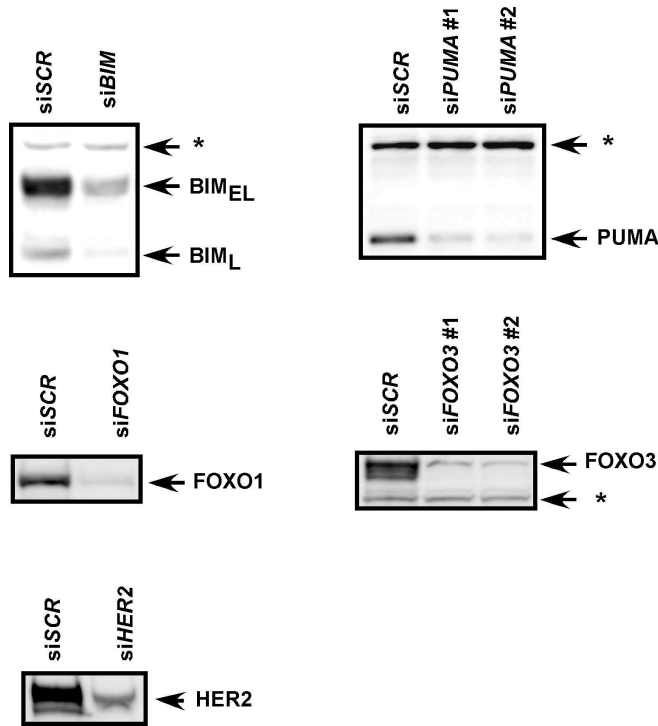


Fig. S2. Immunoblot analysis of siRNA-mediated knockdown. BT474 cells

transfected with the indicated siRNA were immunoblotted with the indicated antibodies (n = 2 independent experiments). Asterisk indicates a cross-reactive band serving as a loading control.

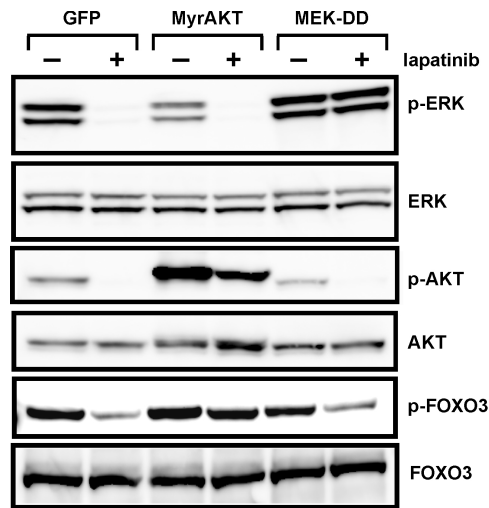


Fig. S3. Regulation of ERK and AKT phosphorylation by constitutively active AKT and MEK. BT474 cells stably expressing GFP, myristoylated AKT (Myr-AKT), or a constitutively active mutant of MEK (MEK-DD) were untreated or treated with lapatinib and immunoblotted with the indicated antibodies (n = 2 independent experiments).

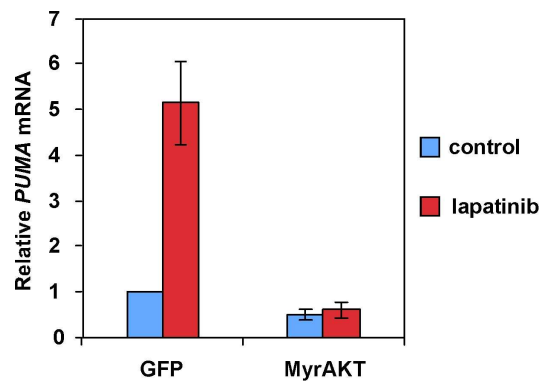


Fig. S4. Inhibition of lapatinib-mediated induction of *PUMA* mRNA by Myr-AKT. *PUMA* mRNA abundance was assessed in the indicated BT474 cells untreated or treated with lapatinib. Data are normalized against GAPDH and presented as mean \pm S.D. of three independent experiments.

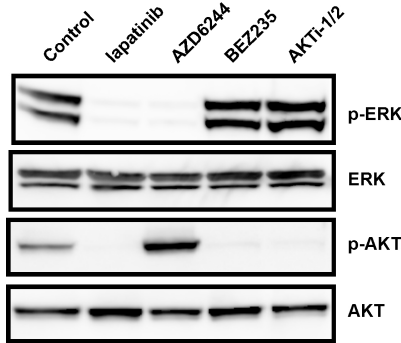


Fig. S5. Inhibition of ERK and AKT phosphorylation by various kinase inhibitors.

BT474 cells were untreated or treated with the indicated kinase inhibitors for 6 hours and immunoblotted with the indicated antibodies (n = 2 independent experiments).

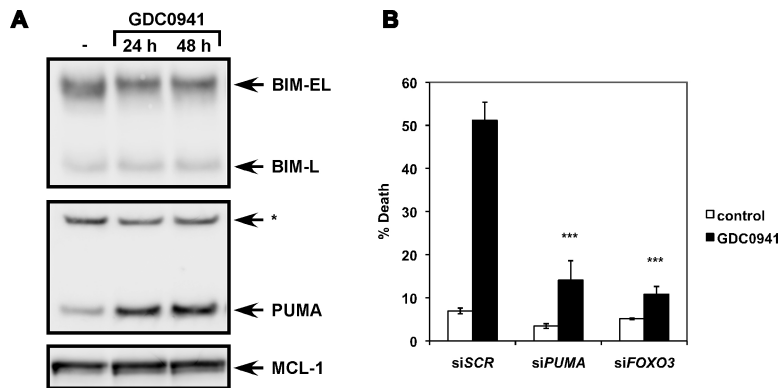


Fig. S6. PUMA is required for GDC0941-induced apoptosis of BT474 cells. (A)

BT474 cells were untreated or treated with GDC0941 and immunoblotted with the indicated antibodies (n = 2 independent experiments). (B) BT474 cells transfected with scramble siRNA (siSCR) or siRNA against *PUMA* or *FOXO3* were untreated or treated with GDC0941. Cell death was quantified by FACS analysis following annexin-V (AV) staining at 36 hours. Data presented are the mean percentage of AV-positive cells \pm SD from three independent experiments. *, $P < 0.05$; **, $P < 0.01$; ***, $P < 0.001$.

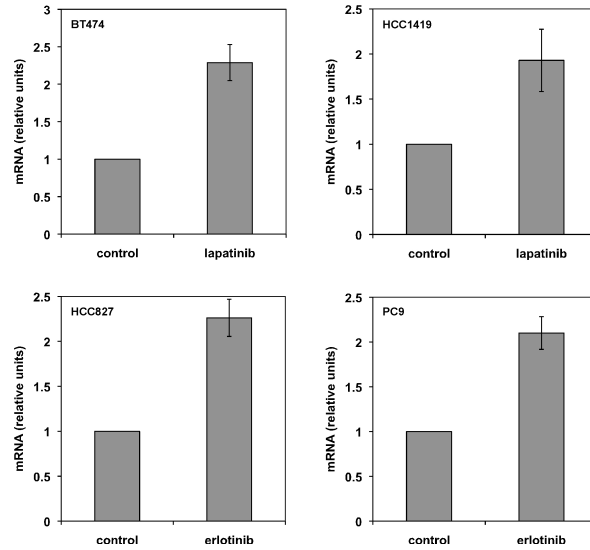


Fig. S7. *BIM* mRNA is induced upon treatment with tyrosine kinase inhibitors. BT474 and HCC1419 cells were untreated or treated with lapatinib for 24 hours. HCC827 and PC9 cells were untreated or treated with erlotinib for 12 and 24 hours, respectively. *BIM* mRNA abundance was assessed by qRT-PCR. Data are normalized against GAPDH and presented as mean \pm S.D. of three independent experiments.

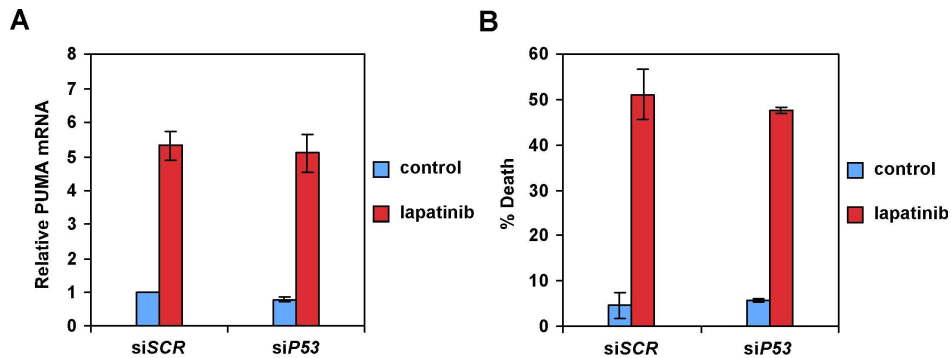


Fig. S8. Knockdown of p53 fails to prevent lapatinib-mediated PUMA induction and apoptosis. (A) *PUMA* mRNA abundance was assessed in BT474 cells that were transfected with scramble siRNA (siSCR) or siRNA against p53 and left untreated or treated with lapatinib for 18 hours. Data are normalized against GAPDH and presented as mean \pm S.D. of three independent experiments. (B) Quantification of cell death by FACS analysis following annexin-V (AV) staining of BT474 cells transfected with scramble siRNA (siSCR) or siRNA against p53 and left untreated or treated with lapatinib for 72

hours. Data presented are the mean percentage of AV-positive cells \pm SD from three independent experiments.

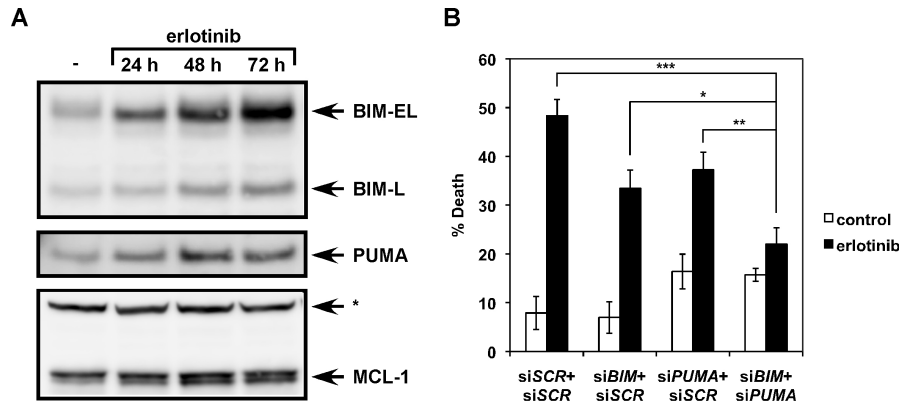


Fig. S9. BIM and PUMA are activated upon erlotinib-induced apoptosis of PC9 cells. (A) PC9 cells, mock treated or treated with erlotinib, were immunoblotted with the indicated antibodies (n = 2 independent experiments). (B) Quantification of cell death by FACS analysis following annexin-V (AV) staining of PC9 cells transfected with scramble siRNA (siSCR) or siRNA against *BIM*, *PUMA*, or both and left untreated or treated with erlotinib for 96 hours. Data presented are the mean percentage of AV-positive cells \pm SD from three independent experiments. *, $P < 0.05$; **, $P < 0.01$; ***, $P < 0.001$.

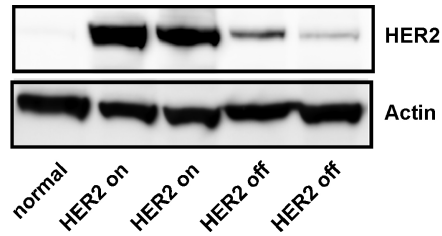


Fig. S10. Immunoblot analysis of HER2 in HER2/Neu-driven mammary tumors.

MTB⁺TAN⁺ female mice were administered doxycycline water to induce HER2. When mice developed tumors measuring 1 cm in the longest dimension, doxycycline was withdrawn for 24 hours to turn off HER2. Tumor lysates were immunoblotted with the indicated antibodies (n = 2 independent experiment). A mammary gland from a mouse that was never given doxycycline served as a control.

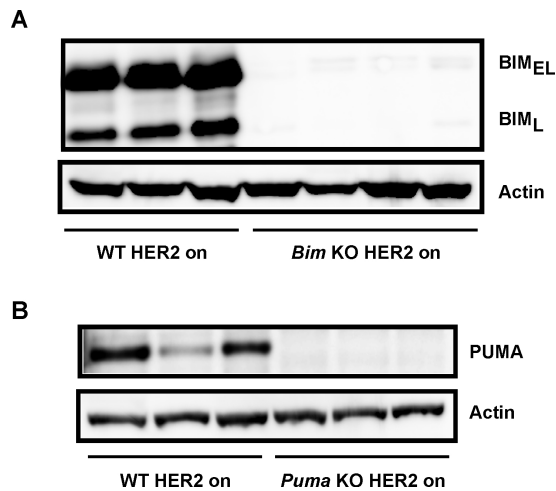


Fig. S11. Immunoblot analysis of BIM and PUMA in HER2/Neu-driven mammary tumors.

(A) Mammary tumors harvested from *MTB⁺TAN⁺* (WT) or *MTB⁺TAN⁺Bim^{-/-}* (*Bim* KO) female mice were immunoblotted with the indicated antibodies (n = 2 independent experiments). (B) Mammary tumors harvested from *MTB⁺TAN⁺* (WT) or *MTB⁺TAN⁺Puma^{-/-}* (*Puma* KO) female mice were immunoblotted with the indicated antibodies (n = 2 independent experiments).

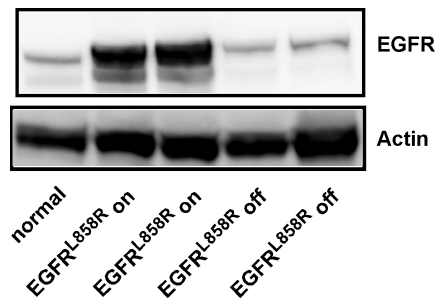


Fig. S12. Immunoblot analysis of EGFR in the tetracycline-inducible EGFR^{L858R} transgenic mouse model. Lung tissue harvested from wild-type mice or *TetO-EGFR^{L858R}; CCSP-rtTA* mice fed with doxycycline-impregnated food or 2 days after doxycycline withdrawal were immunoblotted with the indicated antibodies (n = 2 independent experiments).

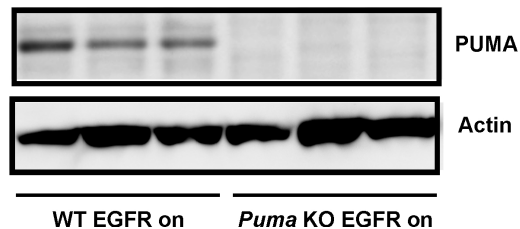


Fig. S13. Immunoblot analysis of PUMA in EGFR^{L858R}-driven mouse lung tumors. Lung tumors harvested from *TetO-EGFR^{L858R}; CCSP-rtTA* (WT) or *TetO-EGFR^{L858R}; CCSP-rtTA; Puma^{-/-}* (*Puma* KO) mice were immunoblotted with the indicated antibodies (n = 2 independent experiments).

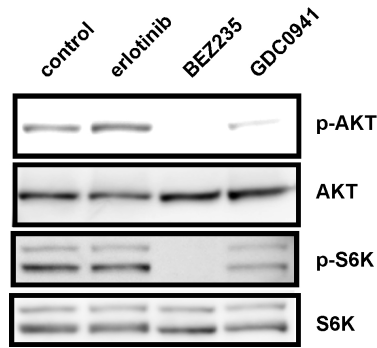


Fig. S14. Immunoblot analysis of phosphorylation of AKT and S6K. HCC1954 cells were untreated or treated with the indicated kinase inhibitors for 6 hours and immunoblotted with the indicated antibodies (n = 2 independent experiments).

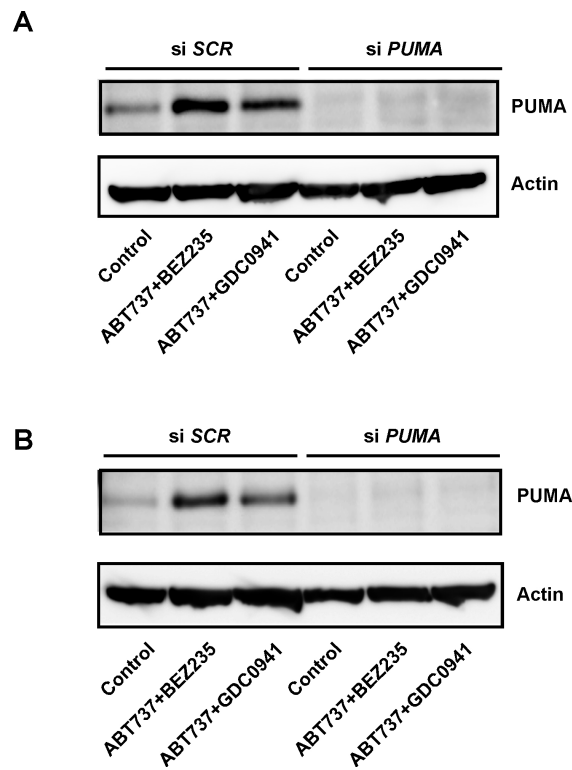


Fig. S15. Immunoblot analysis of siRNA-mediated knockdown of *PUMA*. H1650 (A) or HCC1954 (B) cells, transfected with the indicated siRNA, were left untreated or treated with the indicated inhibitors and immunoblotted with the indicated antibodies (n = 2 independent experiments).